PCCP

Solid state equilibrium in the *n*-alkanols family: the stability of binary mixed samples

L. Ventolà,*[a] T. Calvet,[a] M. A. Cuevas-Diarte,[a] X. Solans,[a] D. Mondieig,[b] P. Négrier[b] and J. C. van Miltenburg[c]

[a] *Departament de Cristal lografia, Mineralogia i Dipòsits Minerals, Facultat de Geologia, Universitat de Barcelona, Martí i Franquès s/n, E-08028, Barcelona, Spain. E-mail: lourdes_ventola@yahoo.com; Fax: (+34)934021340; Tel: (+34)934021350*

[b] *Centre de Physique Moléculaire et Optique Hertzienne, UMR 5798 au CNRS Université Bordeaux I, 351 Cours de la Libération, 33405, Talance, France*

[c] *Chemical Thermodynamics Group, Faculty of Chemistry, Debye Institute, Utrecht University, Padualaan 8, CH-3584, Utrecht, The Netherlands*

Received 23rd October 2002, Accepted 13th January 2003
First published as an Advance Article on the web 23rd January 2003

The stability of binary mixed samples in the normal alkanols family is studied here *via* the $C_{18}H_{37}OH$–$C_{20}H_{41}OH$ and $C_{19}H_{39}OH$–$C_{20}H_{41}OH$ systems. The stability of mixed samples depends on the method used for their preparation. In the samples obtained by the dissolution–evaporation (D + E) method (with diethyl ether), the phases in the solid–solid and solid–liquid equilibria are stable after preparation. However samples obtained by the melting–quenching (M + Q) method (quenching in liquid nitrogen) are only stable for phases in the solid–liquid equilibria. The phases observed in the solid–solid equilibria evolve over time, even after two years' storage at low temperature (279 K).

Introduction

This paper is part of a general study of solid–solid and solid–liquid miscibility in the *n*-alkanols, CH_3–$(CH_2)_{(n-1)}$–OH (abbreviated $C_nH_{2n+1}OH$), family. The study analyses the stability of binary mixed samples in the $C_{18}H_{37}OH$–$C_{20}H_{41}OH$ and $C_{19}H_{39}OH$–$C_{20}H_{41}OH$ systems. This paper is a result of collaboration with the REALM† group (*Réseau Européen sur les Alliages Moléculaires*), which researches the characterisation, fabrication, future possibilities and application of molecular alloys.[1–4] The REALM group has been studying for thirty years several molecular material families with different types of configurations and interactions. Among these families are: the naphthalene derivatives, benzene derivatives, substances with chiral molecules, substances with plastic phases, liquid crystals and *n*-alkanes. The *n*-alkanes family has been studied intensively.[5–8] The *n*-alkanes consist of chains of carbon and hydrogen atoms, in which all the intermolecular interactions are of the van der Waals type. These substances form homologous series, which differ in the number of carbon atoms; their properties alternate according to the parity of the number of carbons in the chain. They are characterised by high latent melting heat, which means that the molecular alloys prepared from them can be used in thermal energy storage. They are described as phase-change materials based on molecular alloys (MAPCM).[2,3]

The reason for studying the *n*-alkanols family is that, although they have the same configuration as the *n*-alkanes family, an –OH group at one end of the chain implies the presence of hydrogen bonds. This fact is related to an increase in the latent heat of fusion. Therefore, the *n*-alkanols could be important for energy storage, providing new MAPCM materials. They also represent a diversification of the intermolecular interactions in fundamental terms.

As REALM research into organic syn-crystallization has revealed stability problems in mixed samples of other substances: normal diacids,[9] paradisubstituted benzenes[10] and *n*-alkanes,[8] we decided to study mixed sample stability phases in the *n*-alkanols family.

In some cases, these phase stability problems are related to the method used to prepare the mixed samples. While the samples were kept at low temperature (279 K), an evolution in the behaviour of the sample could be detected, for example, by DSC. Therefore, two methods were used to prepare mixed samples: dissolution–evaporation (D + E) and melting–quenching (M + Q). The mixed samples were kept at low temperature (279 K) and were periodically examined by DSC, X-ray powder diffraction, Raman scattering and infrared spectroscopy.

The polymorphism of the $C_{18}H_{37}OH$, $C_{19}H_{39}OH$ and $C_{20}H_{41}OH$ is rich and complex.[11] At room temperature two ordered stable phases are observed: γ and β, both monoclinic. The γ phase ($C2/c$, $Z = 8$) is the stable phase for the $C_{18}H_{37}OH$[12,13] and $C_{20}H_{41}OH$,[14] and the β phase ($P2_1/c$, $Z = 8$) is the stable phase for the $C_{19}H_{39}OH$.[11] The γ phase was characterised by an *all-trans* conformation of the C–C bonds in the polymethylene chain. This phase was also seen in other even *n*-alkanols with shorter carbon chains, such as $C_{14}H_{29}OH$[15] and $C_{16}H_{33}OH$.[16] The β phase contains two molecules in the asymmetric unit, each of which is a different rotational isomer. The first isomer is an *all-trans* conformer (similar to the γ phase), while the second isomer has all C–C–C–C torsion angles in *trans* form and the C–C–C–O torsion angle in *gauche* form (COgt-). This phase was observed in other odd *n*-alkanols with shorter carbon chains such as $C_{13}H_{27}OH$, $C_{15}H_{31}OH$ (ref. 17) and $C_{17}H_{35}OH$ (ref. 12).

† REALM consists of four European universities: University of Barcelona, Polytechnic University of Catalonia, University of Utrecht and Bordeaux I University.

On heating, the γ and β phases transform to a monoclinic rotator phase R'_{IV} ($C2/m$, $Z = 4$) at a few degrees below melting point.[11,12] This rotator phase shows COgt- (end *gauche*) forms and a disorder in the carbon chain.[11] For other alkanols with shorter carbon chains, such as $C_{14}H_{29}OH$, $C_{15}H_{31}OH$ and $C_{16}H_{33}OH$, another rotator phase R'_{II} is observed before melting. This is hexagonal with space group $R\bar{3}m$ and six molecules in the unit cell.

Previous studies have reported that the application of the D + E or M + Q method in *n*-alkanol compounds caused differences in the polymorphic behaviour of the even *n*-alkanols.[11] The $C_{18}H_{37}OH$ and the $C_{20}H_{41}OH$ compounds melted and quenched show the metastabilisation of a monoclinic β phase. This phase is isostructural to the one observed at low temperature in the *n*-alkanols with an odd number of carbons,[12] as well as in the even *n*-alkanols with a shorter chain ($C_{12}H_{25}OH$). However, the same compounds after dissolution and solvent evaporation do not change their polymorphic behaviour (*i.e.* the phase observed at low temperature is γ).

Experimental section

The *n*-alkanols, $C_nH_{2n+1}OH$, with *n* from 18 to 20, were purchased from Fluka Chemica with a stated purity of more than 98%. They were used without further purification.

The mixed samples were obtained either by the dissolution–evaporation (D + E), or the melting–quenching (M + Q) method. In the D + E method the components are weighed in the desired proportions and dissolved with diethyl ether. The solvent is then evaporated. In the M + Q method the components are weighed in the desired proportions, melted and mixed to give a homogeneous sample, and then quenched into liquid nitrogen.

The mixed samples were characterised as follows:

Differential scanning calorimetry (DSC)

Calorimetric measurements were made with a Perkin–Elmer DSC-7 calorimeter. Sealed aluminium pans (with sample weights between 3.9 and 4.1 mg) were heated to a melting point, cooled and reheated, at 2 K min^{-1}. The temperature range scanned was from 273 K to the liquid phase. The instrument was calibrated with the known melting temperature and enthalpy of fusion of indium and melting temperature of *n*-decane. Random uncertainties were estimated using the student's test, with a 95% threshold of reliability. The systematic uncertainties of temperatures and heat-flow calibration coefficient for the DSC were estimated as ±0.2 K and 2%, respectively.

X-ray powder diffraction analysis (XRD)

A Siemens D-500 diffractometer was used with Bragg-Brentano geometry, using Cu Kα radiation and secondary monochromator. The data were collected at different temperatures using an Anton PAAR TTK camera with a heating rate of 0.02 K· sec^{-1} and 5 min of stabilisation time. The analysis was performed in a heating process from 298 K to the melting temperature. The patterns were scanned with a step size of 0.025°, step time of 5 sec and 2θ range of 1.6–60°.

Raman scattering

Polarised Raman spectra were taken on powdered samples, using a Jobin Yvon T64000 spectrometer and argon-ion laser excitation. A Control Data CDC detector was used. The spectra were recorded with the 514.5 nm line with a light power equal to 3.30 W. All spectra were calibrated against selected neon lines. The measured range was 17.5–1700 cm^{-1}. All spectra were measured at 298 K in a macro-Raman spectrometer. The measurements for the mixed samples obtained by M + Q were taken immediately and two years after the sample preparation. The position, half width, and relative intensity of each peak were determined, assuming a Lorentzian function (the Gaussian contribution is negligible).

Infrared spectroscopy (IR)

The infrared spectra were recorded by a Bomem DA 3FTIR spectrometer. All samples were finely powdered and measured at room temperature using a diffuse reflection accessory (DRIFT), with a range of 450–4000 cm^{-1}. The resolution was 4 cm^{-1}. All spectra were run using the vacuum mode. The detector used was MCTT (wide range) ; the beam splitter was KBr and the source a glow bar. Each spectrum was obtained by averaging 100 scans. The mixed samples obtained by M + Q were measured immediately and two years after the sample preparation.

Results and discussion

For every binary system, many compositions have been studied. However, this article focuses on the equimolarity of each system, as this is the most significant composition.

$0.50C_{18}H_{37}OH$–$0.50C_{20}H_{41}OH$

Samples obtained by the M + Q method. *First heating.* The DSC curve obtained with a fresh sample just after its elaboration (Fig. 1(M + Q immediate)) shows:

(i) A first signal, less energetic as a result of solid–solid transitions (Fig. 1a). This signal, according to X-ray powder diffraction results, corresponds to the following phase domain sequence: $[\beta] \rightarrow [\beta + R'_I] \rightarrow [R'_{II}]$. The β, R'_I(orthorhombic) and R'_{II} phases are metastable phases in $C_{18}H_{37}OH$ and $C_{20}H_{41}OH$.

(ii) A second signal, more energetic, corresponding to the melting phenomenon $[R'_{II}] \rightarrow [L]$ (Fig. 1b). X-ray powder diffraction showed that it is the R'_{II} phase which melts.

By monitoring samples after they were kept for 717 days at low temperature (279 K), we observe [Fig. 1 (M + Q 717 days at 279 K)] the following:

(i) The DSC signal, for the solid–solid transitions (Fig. 1a) moves towards higher temperatures. And a new signal, not very energetic, appears around 321 K. By X-ray powder diffraction, this new signal cannot be assigned to any phase transition. The same phase R'_{II} is observed before and after the signal.

(ii) For the melting signal (Fig. 1b) no significant differences were observed (their deviations are inside the error bars).

The same behaviour was observed in other compositions of the system, such as $0.80C_{18}H_{37}OH$–$0.20C_{20}H_{41}OH$ and $0.30C_{18}H_{37}OH$–$0.70C_{20}H_{41}OH$. However, for the richest compositions in one of the original compounds, no displacements were noticed in the DSC signals for the solid–solid transitions.

If we try to draw an experimental phase diagram with the results obtained for this and other compositions studied, we obtain a diagram which is incoherent in thermodynamic terms. A $[\beta + R'_I]$ domain that can not be closed is observed. Although the beginning of the DSC signals seems to show the existence of a minimum for the $[\beta + R'_I]$ domain, the end of these signals does not manage to close it. This, along with the evolution of the DSC signals corresponding to the solid–solid transitions, justifies the following hypothesis: the phases involved in the solid–solid transition of the samples obtained by the M + Q method are not stable even after having been stored at 279 K for two years.

Second heating. The DSC curve is very similar to those obtained during the first heating of the sample, when the heating takes

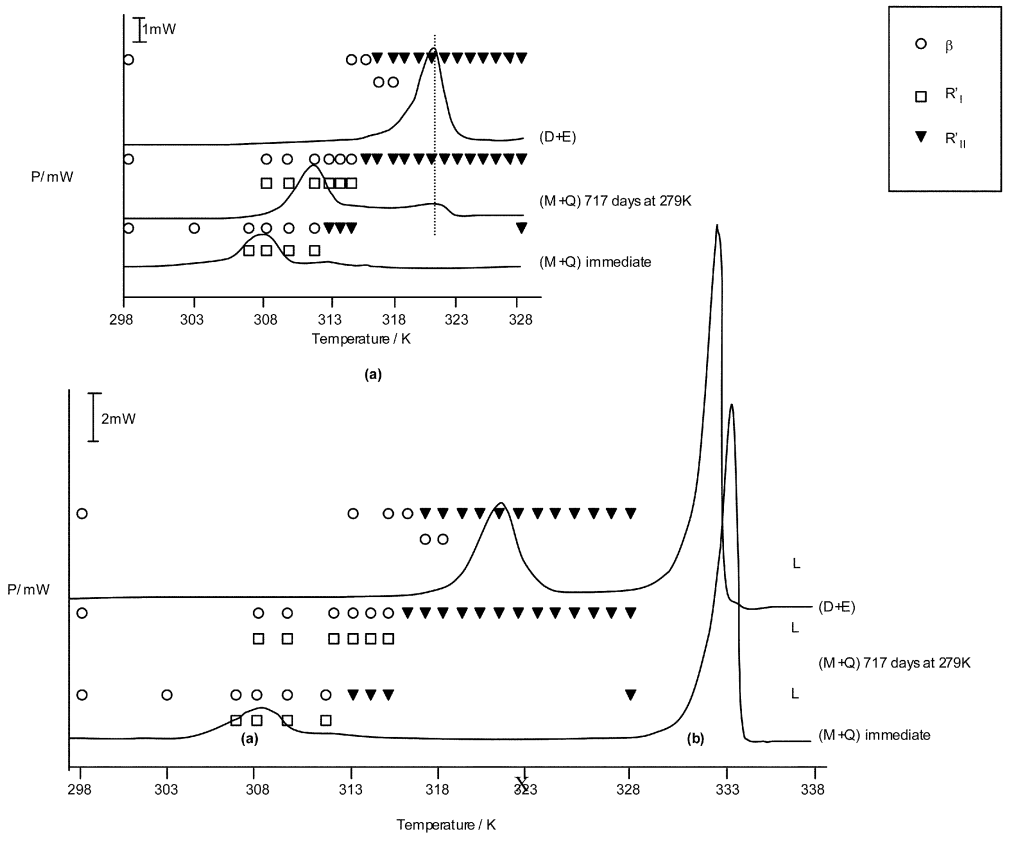

Fig. 1 $0.50C_{18}H_{37}OH$–$0.50C_{20}H_{41}OH$ samples obtained by D + E and M + Q methods; DSC diagrams (first heating) and the symbols for X-ray powder diffraction results.

place immediately after its preparation. This is not surprising, as the M + Q method involves the sample melting. The differences observed in the signal forms may be explained by different sample distributions in the DSC crucible before and after the liquid state.

However, differences can be observed for the solid–solid transition temperatures when comparing this second heating signal with the signal obtained for the first heating run after the sample has been stored for two years at 279 K. No differences were observed in the melting phenomenon.

Samples obtained by the D + E method. *First heating.* As in the sample obtained by the M + Q method, two signals were observed in the DSC curves [Fig. 1(D + E)]:

(i) One less energetic signal, as a result of solid–solid transitions (Fig. 1a). However, in this case, the signal does not move over time towards higher temperatures. X-ray diffraction showed that this is due to the following phase domain sequence: $[\beta] \rightarrow [\beta + R'_{II}] \rightarrow [R'_{II}]$. There was no R'_I phase.

(ii) The other signal is more energetic, corresponding to the melting phenomenon $[R'_{II}] \rightarrow [L]$ (Fig. 1b). In this case, the melting phase is also R'_{II}.

The main issue is that the DSC signal, corresponding to the phenomenon that appears for the samples obtained by the M + Q method and maintained for a long time at 279 K, coincides in temperature with the solid–solid transitions for the sample obtained by the D + E method [Fig. 1a(M + Q 717 days at 279 K and D + E)]. This confirms the previous hypothesis: the phenomenon that appears over time in samples obtained by the M + Q method determines the end of the evolution. No significant differences in the melting phenomenon were found between samples obtained by the two methods (Fig. 1b). The same phase, R'_{II}, was observed.

Second heating. The DSC curves are comparable to those samples obtained by the M + Q method.

For the β phase observed at room temperature in the samples obtained by the M + Q and D + E methods, no differences were detected by X-ray powder diffraction analysis.

However, a detailed study by Raman and IR spectroscopy showed small differences between the samples obtained by the two methods. The vibration mode assignments of the Raman spectra were made using the analogy to the spectra of the components,[11] the basis of the vibrational spectra studies for the *n*-alkanes[18–21] and the crystal structures of the *n*-alkanols.[12–14]

Fig. 2 shows the Raman spectra for the main frequencies of phonon modes in the 800–1550 cm^{-1} range for the mixed samples and components. As shown, there are no significant differences between the mixed samples obtained by different methods. In the CH_2 rocking mode zone ($700 < \nu < 1000$ cm^{-1}), bands that are attributed to movements at the ends of the chains can be observed, according to Snyder.[19,20] In all the spectra, a band (at 890 cm^{-1}) attributed to CH_3 rocking of a chain with *all-trans* conformation in the *n*-alkanes was observed. In the spectra of the mixed crystals and the $C_{19}H_{39}OH$ a band at 875 cm^{-1} was observed, which was assigned in ref. 11 to COgt- (end *gauche*) mode observed in the β-form of this family of substances. The bands assigned by Snyder[19,20] to kink defects (CC–gtg′- at 850 cm^{-1}) and end *gauche* defects (CCgt- at 870 cm^{-1}), were not detected neither in the original compounds, nor here.

No significant differences were observed in the C–C stretching bands ($1000 < \nu < 1150$ cm^{-1}), CH_2 wagging/twisting bands ($1150 < \nu < 1400$ cm^{-1}) or CH_2 scissoring bands ($1400 < \nu <$ 1500 cm^{-1}) between the mixed crystals and the β and γ-forms of the original compounds.

Nevertheless, great differences were observed in the IR spectra between the mixed samples obtained by different methods. Fig. 3(a, b, c) shows the IR spectra at 298 K for the mixed sample obtained by the D + E method, the mixed sample

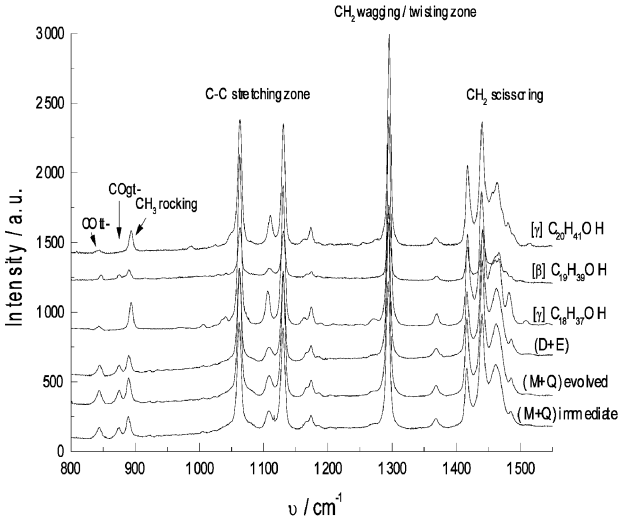

Fig. 2 The 800–1600 cm^{-1} range of Raman scattering at 298 K for the $C_{20}H_{41}OH$, $C_{19}H_{39}OH$, $C_{18}H_{37}OH$; mixed samples obtained by D + E method (D + E), by M + Q method measured after 720 days [(M + Q) evolved], and by M + Q measured immediately [(M + Q) immediate].

obtained by the M + Q method measured immediately (M + Q immediate), measured two years after the sample preparation (M + Q evolved), and the spectra of pure substances.

The following main differences were observed:

— In the frequency region of $\nu < 650$ cm^{-1}, the intensity of modes 505, 527, and 542 cm^{-1} is a function of the method followed to obtain the mixed sample. The bands at 505 and 527 cm^{-1} are stronger in the M + Q mixed sample analysed just after its preparation (M + Q immediate). The band at 542 cm^{-1} is stronger in the D + E mixed sample and its IR spectra are similar to the IR spectra of the β-form of $C_{19}H_{39}OH$. The intensities in the M + Q evolved mixed sample are intermediate between the M + Q immediate and the D + E mixed samples. According to Snyder,[19,20] in this zone the modes of C–C stretching and C–C–C bending contribute more or less equally to the intensity of bands, but above 650 cm^{-1} the C–C–C bending mode contributes more to potential energy. As no significant differences are observed above 650 cm^{-1}, these intensity differences between the bands of alloys can be assigned to C–C–C bending, as well as to the differences in the packing of the chains.

— There is a variation of the splitting in the bands of the CH_2 rocking (~720 cm^{-1}) and CH_2 scissoring (~1470 cm^{-1}). These bands show splitting in the β and γ phases of the original compounds and in the mixed samples obtained by the D + E method (Fig. 3a and 3b). This splitting decreases in the M + Q mixed samples, mainly in the M + Q immediate alloy. This phenomenon was also observed in the mixed samples of *n*-alkanes[22] and the absence of this splitting, especially in the CH_2 scissoring band, was attributed to the domain size. The increase in splitting occurs when the domain sizes are increased. These "domains" might be more appropriately referred to as "percolation cluster".

— In the frequency region of CH_2 rocking ($1000 > \nu > 700$ cm^{-1}) and CH_2 wagging/twisting ($1150 > \nu > 1400$ cm^{-1}), new bands appear between the k-odd modes in the spectra of the mixed samples similar to the spectra of β-form of $C_{19}H_{39}OH$. Since the k-even modes are IR inactive for the *all-trans* chain, these bands must result from a non-planar conformation, that confirms the typical *gauche* form of the β-phase.

— A variation in the intensity of the bands at 1060, 1080, 1107 and 1124 cm^{-1} was observed in the spectra of the three mixed samples (Fig. 3a). The β-phase of $C_{19}H_{39}OH$ shows the same bands.

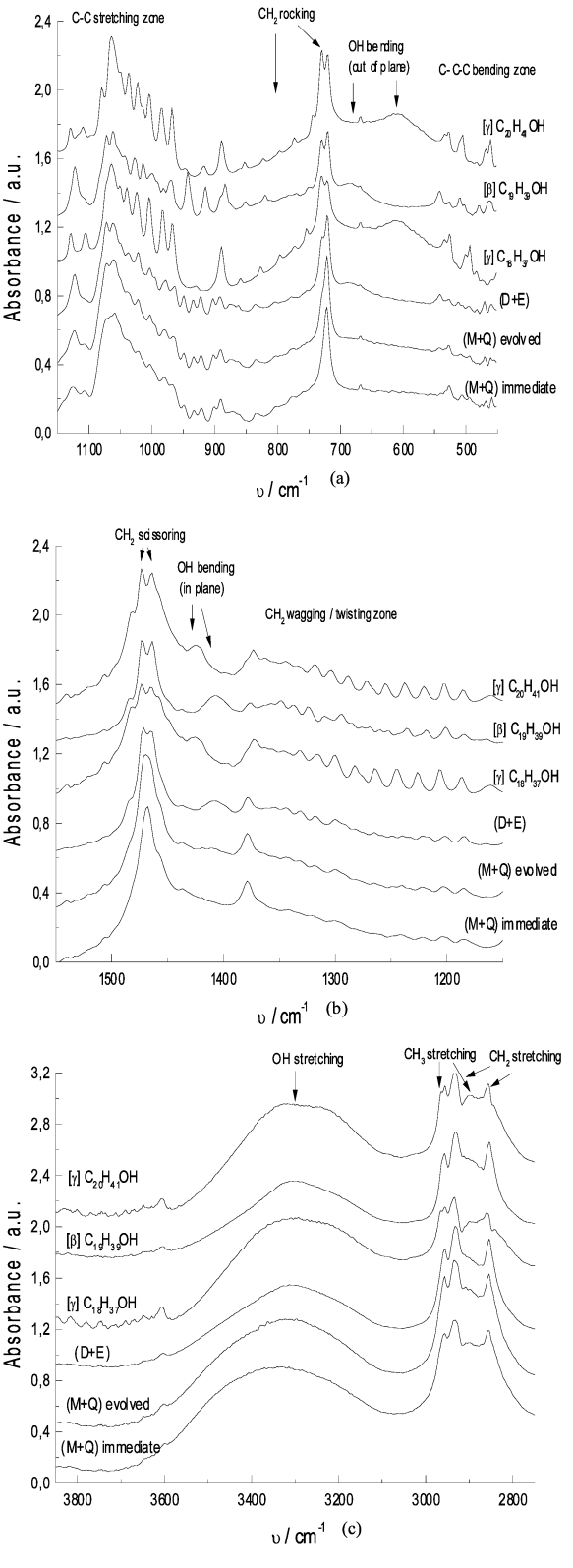

Fig. 3 Main zones of infrared spectra: (a) $1150 \geq \nu \geq 450$ cm^{-1}, (b) $1600 \geq \nu \geq 1100$ cm^{-1}, (c) $3850 \geq \nu \geq 2750$ cm^{-1} at 298 K for the $C_{20}H_{41}OH$, $C_{19}H_{39}OH$ and $C_{18}H_{37}OH$ mixed samples obtained by the D + E method (D + E), by the M + Q method measured after 720 days [(M + Q) evolved] and by the M + Q measured immediately [(M + Q) immediate].

The band at 1080 cm^{-1} was observed in polyethylenes. According to the potential energy distribution computed by Snyder,[20] this band is best described as C–C stretching mode. However, as it also has a significant contribution from CH_2 wagging, is attributed by Snyder to anti-symmetrical C–C

stretching caused by the wagging of the methylene group adjoining the *gauche* bond. The 1107 and 1124 cm^{-1} were also attributed to end-*gauche* defect of the chains.

— The OH bending out-of-plane and in-plane modes of the D + E mixed samples are the same as those observed in the β-phase of $C_{19}H_{39}OH$. These modes are not clearly observed in the M + Q immediate mixed samples, while they are observed in the M + Q evolved mixed samples, mainly the OH bending in-plane.

— The frequency and the full-width at half maximum of OH stretching (Fig. 3c) change from 3325 cm^{-1} (full-width 367) for the M + Q immediate mixed samples to 3316 cm^{-1} (full-width 344) for the M + Q evolved mixed samples and to 3302 cm^{-1} (full-width 314) for the D + E mixed samples. The latter is similar to the β-phase of $C_{19}H_{39}OH$.

The results obtained from Raman scattering and IR spectroscopy are consistent with those obtained from X-ray powder diffraction. It was confirmed that the D + E and M + Q mixed samples show a β-phase with two chain-types, one with an *all-trans* conformation and the other with the *gauche* form for CCCO moiety. The results of IR spectroscopy showed that the β-form of D + E mixed samples was more like to the β-form of the $C_{19}H_{39}OH$, while the M + Q mixed samples showed a greater number of structural defects, located in the position of the oxygen atom and the hydrogen bonds. In consequence, differences in the packing of the chains and in the domain size were observed between the D + E and M + Q mixed samples. These differences in the M + Q mixed samples tended to disappear over time (more than two years after the mixed sample preparation).

$0.50C_{19}H_{39}OH$–$0.50C_{20}H_{41}OH$

Samples obtained by the M + Q method. *First heating.* In this system, two different signals were also observed in DSC analysis (Fig. 4):

(i) The less energetic signal, corresponding to the solid–solid transitions (Fig. 4a). In this case, it is a result of the following sequence of phase domains: $[\beta] \rightarrow [\beta + R'_I] \rightarrow [R'_I + R'_{IV}] \rightarrow [R'_{IV}]$. Where β is stable in the $C_{19}H_{39}OH$ and metastable in the $C_{20}H_{41}OH$, R'_I is metastable in the two original compounds, and R'_{IV} is stable in both compounds.

(ii) The most energetic signal, corresponding to the melting phenomenon $[R'_{IV}] \rightarrow [L]$ (Fig. 4b). Here, the melting phase is R'_{IV}.

In all compositions of this system, no signal evolution is observed in the DSC signals corresponding to the solid–solid transitions, no matter how long the samples are kept at low temperature (279 K). However, there are some common points with the previous binary system:

(i) A low energy phenomenon at the end of the first signal. Using X-ray powder diffraction, it was not possible to assign this phenomenon to any phase transition: the same phase (R'_{IV}) was observed before and after.

(ii) The existence of R'_I phase.

(iii) The experimental phase diagram based on the results from this and other system compositions is incoherent in thermodynamic terms. Once again, it is not possible to close the $[\beta + R'_I]$ domain.

Second heating. There are no differences between the first and second heating.

Samples obtained by D + E method. *First heating.* The DSC signal for the solid–solid transitions coincides in the same position as the low energy phenomenon observed at the signal end in the samples obtained by M + Q method. The R'_I phase was not observed. In fact, the situation is similar to the $C_{18}H_{37}OH$–$C_{20}H_{41}OH$ system.

Second heating. As in the previous system, the DSC diagram corresponds to that obtained from the M + Q samples.

In this system, as in the $C_{18}H_{37}OH$–$C_{20}H_{41}OH$ system, whith X-ray powder diffraction differences in the β phase between the samples obtained by M + Q and by D + E could not be detected. Only IR spectroscopy showed small differences in the C–C–C bending zone (Fig. 5) between the samples obtained by the two methods.

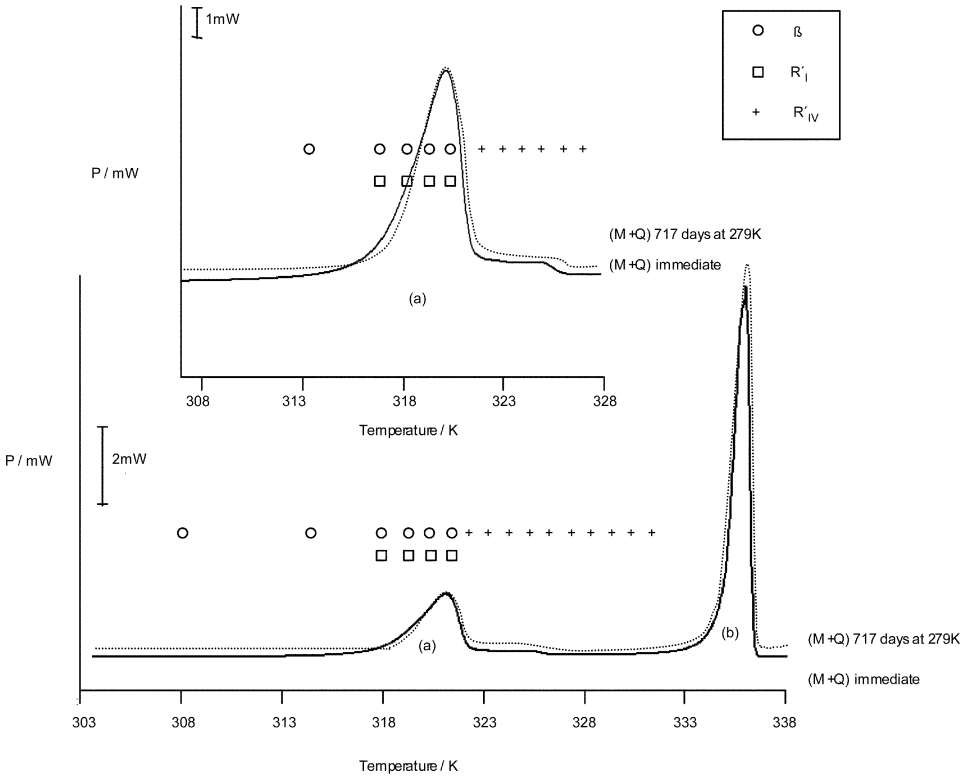

Fig. 4 $0.50C_{19}H_{39}OH$–$0.50C_{20}H_{41}OH$ sample obtained by M + Q method; DSC diagrams (first heating) and the symbols corresponding to X-ray powder diffraction results.

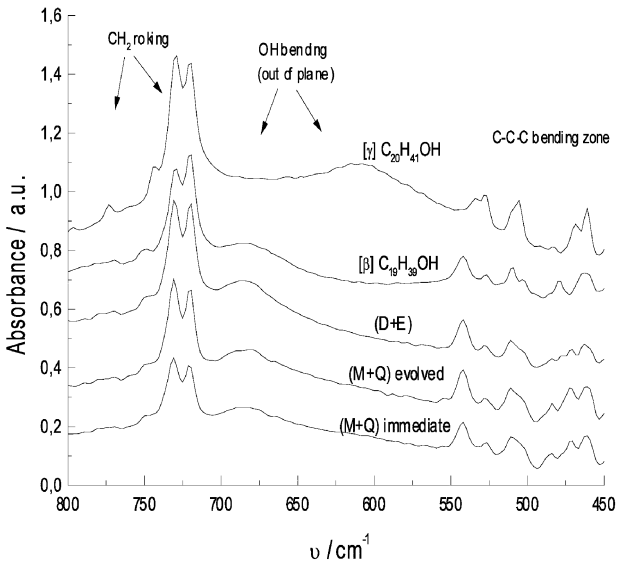

Fig. 5 The 800–450 cm^{-1} range of infrared spectra at 298 K for $C_{20}H_{41}OH$, $C_{19}H_{39}OH$, mixed samples obtained by the D + E method (D + E), by the M + Q method measured after 745 days [(M + Q) evolved] and by the M + Q measured immediately [(M + Q) immediate].

Conclusions

The stability of samples depends on which method (*i.e.* D + E or M + Q) is used. The dissolution–evaporation (D + E) method (using diethyl ether as solvent) allows to obtain stable samples. In this case, the phases involved in the solid–solid and solid–liquid equilibria are stable after the preparation of the samples. However, in the case of samples obtained by the melting–quenching (M + Q) method (quenched in liquid nitrogen), only the phases involved in the solid–liquid equilibria are stable. The phases observed in the solid–solid equilibria evolve over time, even up to two years after the sample's storage at low temperature (279 K).

Solid state miscibility shows metastable forms in the original compounds. The β phase observed in mixed compositions of both systems at room temperature is stable in odd *n*-alkanols and even *n*-alkanols with a shorter carbon number. Only a detailed study by Raman and IR spectroscopy permits us to detect small differences. The results of IR spectroscopy show that the β-form of D + E mixed samples is more like the β-form of $C_{19}H_{39}OH$, while the M + Q mixed samples show a greater number of structural defects in the oxygen atom position. These structural defects and differences in the hydrogen bonds, as a consequence of the packing of the chains, were observed in the D + E and M + Q mixed samples. On heating, these two "types" of β phase behave differently: the stable β phase of the D + E mixed samples transforms directly to R'_{II} rotator phase and then melts, whereas the metastable β phase of the M + Q mixed samples first transforms to a metastable R'_{I} rotator phase before transforming to R'_{II} stable phase.

Acknowledgements

This study was financially supported by the CICYT (project number MAT 97-0371) and the Generalitat de Catalunya (Grup consolidat 1996SGR0039 and Xarxa Temàtica Aliatges Moleculars).

References

1 M. A. Cuevas-Diarte, N. B. Chanh and Y. Haget, *Mater. Res. Bull.*, 1987, **22**, 985–994.
2 Y. Haget, D. Mondieig and M. A. Cuevas-Diarte, Molecular Fr 91/08695 Patent–France, 1991.
3 Y. Haget, *J. Chim. Phys.*, 1993, **90**, 313.
4 M. A. Cuevas-Diarte, T. Calvet, J. Ll. Tamarit, D. Mondieig and H. A. J. Oonk, *Mundo Científico*, 2000, **213**, 45–49.
5 P. Espeau, *PhD Thesis*, Université Bordeaux I, France, 1995.
6 L. Roblès, *PhD Thesis*, Université Bordeaux I, France, 1995.
7 F. Rajabalee, *PhD Thesis*, Université Bordeaux I, France, 1998.
8 V. Metivaud, *PhD Thesis*, Université Bordeaux I, France, 1999.
9 M. A. Cuevas Diarte, *PhD Thesis*, Universitat de Barcelona, Spain, 1980.
10 L. Ventola, Bachelorship project, Universitat Autònoma de Barcelona, 1997.
11 L. Ventola, M. Ramírez, T. Calvet, X. Solans, M. A. Cuevas-Diarte, N. Negrier, D. Mondieig, J. C. van Miltenburg and H. A. J. Oonk, *Chem. Mater.*, 2002, **14**, 508–517.
12 T. Seto, *Mem. Coll. Sci. Kyoto Univ.*, 1962, **A30**, 89–107.
13 K. Fujimoto, T. Yamamoto and T. Hara, *Rep. Prog. Polym. Phys. Jpn.*, 1985, **28**, 163.
14 F. Michaud, L. Ventola, T. Calvet, M. A. Cuevas-Diarte, X. Solans and M. Font-Bardia, *Acta Crystallogr., Sect. C: Cryst. Struct. Commun.*, 2000, **56**, 219.
15 D. Precht, *Fette Seifen Anstrichm.*, 1976, **5**, 189.
16 S. Abrahamsson, G. Larsson and E. von Sydow, *Acta Crystallogr.*, 1960, **13**, 770.
17 M. Ramírez, *PhD Thesis*, Universitat de Barcelona, Spain, 2002.
18 M. Maroncelli, S. P. Qi., H. L. Strauss and R. G. Snyder, *J. Am. Chem. Soc.*, 1982, **104**, 6237.
19 R. G. Snyder and J. H. Schachtschneider, *Spectrochim. Acta*, 1963, **19**, 85; J. H. Schachtschneider and R. G. Snyder, *Spectrochim. Acta*, 1963, **19**, 117.
20 R. G. Snyder, *J. Chem. Phys.*, 1967, **47**, 1316.
21 G. Zerbi, R. Magni, M. Gussoni, K. H. Moritz, A. Bigotto and S. Dirlikov, *J. Chem. Phys.*, 1981, **75**(7), 3175.
22 R. G. Snyder, M. C. Goh, V. J. P. Srivatsavoy, H. L. Strauss and D. L. Dorset, *J. Phys. Chem.*, 1992, **96**, 10 008.